Available online at www.sciencedirect.com
SCIENCE DIRECT®
Journal of Sound and Vibration 285 (2005) 653–667
JOURNAL OF SOUND AND VIBRATION
www.elsevier.com/locate/jsvi

A stable adaptive neural-network-based scheme for dynamical system control

X. Xu[a,b], Y.C. Liang[c,d,*], H.P. Lee[d,e], W.Z. Lin[d], S.P. Lim[e], X.H. Shi[c]

[a]*College of Mathematics, Jilin University, 10 Qian Wei Road, Changchun 130012, People's Republic of China*
[b]*Institute of Vibration Engineering Research, Nanjing University of Aeronautics and Astronautics, Nanjing 210016, People's Republic of China*
[c]*College of Computer Science and Technology, Jilin University, 10 Qian Wei Road, Changchun 130012, People's Republic of China*
[d]*Institute of High Performance Computing, 1 Science Park Road, #01-01 The Capricorn, Singapore Science Park II 117528, Singapore*
[e]*Department of Mechanical Engineering, National University of Singapore, 9 Engineering Drive 1 119260, Singapore*

Received 13 November 2003; received in revised form 17 May 2004; accepted 26 August 2004
Available online 10 December 2004

Abstract

A stable adaptive neural-network-based control scheme for dynamical systems is presented and a continuous recurrent neural network model of dynamical systems is constructed in this paper. A novel algorithm for updating weights in the neural network, which is not derived from the conventional back propagation algorithm, is also constructed. The proposed control law is obtained adaptively by a continuous recurrent neural network identifier, but not by a conventional neural network controller. In such a way, the stability in the sense of the Lyapunov stability can be guaranteed theoretically. The control error converges to a range near the zero point and remains within the domain throughout the course of the execution. Numerical experiments for a longitudinal vibration ultrasonic motor show that the proposed control scheme has good control performance.

*Corresponding author. College of Computer Science and Technology, Jilin University, 10 Qian Wei Road, Changchun, 130012, People's Republic of China. Tel.: +86 431 5168510; fax: +86 431 5166063.
E-mail address: liangyc@ihpc.a-star.edu.sg (Y.C. Liang).

0022-460X/$ - see front matter © 2004 Elsevier Ltd. All rights reserved.
doi:10.1016/j.jsv.2004.08.034

1. Introduction

Adaptive control of dynamical systems has been an active area of research for many years. Most of the problems were solved for the adaptive control of linear systems. Recent advances in nonlinear control theory have inspired the development of adaptive control schemes for nonlinear plants [1,2]. A common assumption of adaptive control schemes is that either all or parts of the system dynamics are known. Therefore, most of the general problems of controlling a totally unknown system cannot even be attempted using conventional control methods.

An obvious solution to overcome the problem is to introduce identification techniques in the control algorithm. The problem of identification consists of choosing an appropriate identification model and adjusting its parameters such that the response of the model to an input is the same as the original system. Following the development of artificial neural network (ANN), the identification schemes based on ANN have become one of the main methods. An ANN is modeled simulating the biological neural networks in the brain and consists of a number of neurons and weighted links. The ANN has a good capability for parallel computation, fault tolerance and mapping approximation [3]. It has been applied widely in the field of modeling, identification and control of dynamical systems, computational mechanics, and many others [4–13].

Stabilization is a key problem in the analysis and design of control systems. An appropriate feedback law should be designed to render the system stable. Due to external disturbances, as well as modeling errors, the conventional training algorithm of ANN, such as the back-propagation algorithm [14], experiences great difficulty in rendering the system stable. Furthermore, conventional control methods using ANN usually need two structures of the ANN [4,14–16]. Such structures bring down the speed of convergence. So, it is very difficult to achieve a stable and on-line control using the conventional ANN methods.

In recent years, some neural network methods based on the Lyapunov stability theorem have been proposed [17–19]. These methods can make the system stable even if the real systems are contaminated with noise or there exists uncertainty in system parameters or dynamics. But existing results are constrained to a certain system class and also suffer from the need of imposing additional restrictions to the currently available scheme. Usually these imposed restrictions cannot be satisfied in real systems, and applied in real world. How to construct a practicable scheme using neural network to adaptively stabilize unknown nonlinear systems has a strong theoretical as well as practical importance when there exist external disturbances and uncertainty in system parameters or systems.

This paper proposes a practical control method using neural network to adaptively stabilize nonlinear dynamical systems. A continuous model of recurrent neural network is constructed to identify the dynamical system. In order to guarantee stability, a novel algorithm for updating the weights of the neural network is provided. The proposed control law is obtained adaptively by the continuous recurrent neural network identifier but not by a conventional neural network controller, which theoretically guarantees the stability in the sense of the Lyapunov stability. The control error converges to a range near the zero point and keeps within this range throughout the execution. The proposed networks are applied to the identification and speed control of an ultrasonic motor (USM).

An USM is a newly developed motor. It is a device that transforms vibration and wave motions of solids into progressive or rotational motions by means of contact frictional forces. The USM has some excellent performances and useful features, such as high torque at low speeds, compactness in size, no electromagnetic interference, short start–stop times, and many others. Owing to the advantages mentioned above, the USM has been used in many practical applications [20–22], such as MEMS, robots, medical instruments, cameras and aeronautics.

The USM is a peculiar motor whose driving principle is different from that of other electromagnetic-type motors, and its characteristics have not been elucidated in detail. It has strong nonlinear speed characteristics that vary with the driving frequency, voltage, load, the temperature and many other factors. It is therefore difficult to construct a precise and practical application model for the USM. In recent years, some models of the USM have been proposed [23,24], but most models are too complex to apply to practical applications. Therefore, it is also difficult to control the USM using the conventional algorithms.

In this paper, numerical simulations are performed using the proposed stable adaptive neural method for the speed control of a longitudinally vibrating USM. Numerical experiments show that the proposed control scheme has good stable performance subject to external disturbances and uncertainty in the USM.

2. Problem statements

From the control designer's point of view, it is difficult to realize a theoretical analysis of nonlinear dynamical systems, and sometimes it is also unnecessary to construct a complex model of nonlinear dynamical systems. A neural network model is proposed in this paper to approximate the nonlinear input–output mapping of the systems. The complex theoretical analysis of the operational mechanism and exact mathematical description of dynamical systems are avoided in the model and the unique requirement for the system is the input–output information.

A three-layer neural network with m input neurons, n hidden neurons and one output neuron is shown in Fig. 1. It has a diagonal structure in the hidden layer, that is, there are no interactions among different hidden neurons, which are shown using dashed lines in Fig. 1. The mathematical description of the model is given by [14]

$$\begin{aligned} x_j(k) &= \sum_i b_{ji}(k)u_i(k) + a_j(k)s(x_j(k-1)), \quad j = 1, 2, \ldots, n, \\ y(k) &= \sum_j p_j(k)s(x_j(k)), \end{aligned} \tag{1}$$

where $x_j(k)$ represents the input of the jth hidden neuron in time k, $u_i(k)$ the ith control input, $a_j(k)$, $b_{ji}(k)$ and $p_j(k)$ represent the self-recurrent weights of hidden neurons, the weights between the input and hidden layer and the weights between the hidden and output layer, respectively. The hyperbolic tangential function $s(x) = (1 - e^{-x})/(1 + e^{-x})$ is selected as the activation function of the hidden neurons.

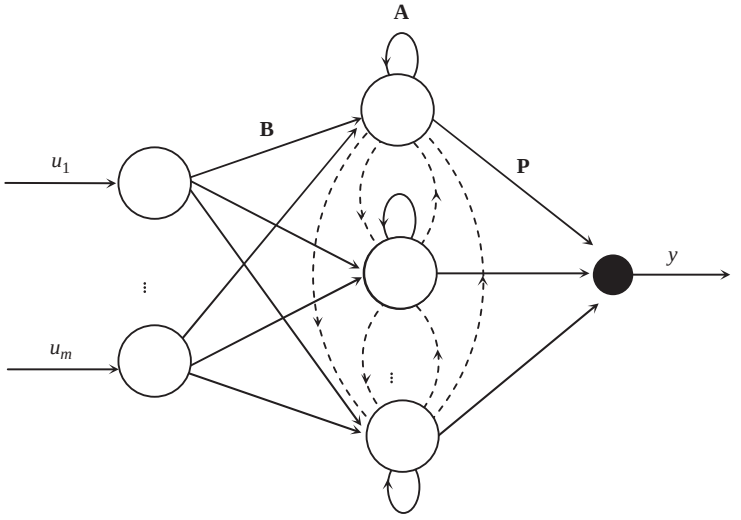

Fig. 1. Architecture of diagonal recurrent neural network in hidden layer.

Supposing that the sampling interval ΔT is small enough, Eq. (1) can be written as

$$\dot{x}_j = -dx_j + A_j s(x_j) + \sum_i B_{ji} u_i, \quad j = 1, 2, \ldots, n,$$
$$y(k) = \sum_j p_j(k) s(x_j(k)), \tag{2}$$

where $d = 1/\Delta T$, $B_{ji} = b_{ji}/\Delta T$ and $A_j = a_j/\Delta T$. Eq. (2) can be written in a matrix form as

$$\dot{\mathbf{x}} = -\mathbf{D}\mathbf{x} + \mathbf{A}\mathbf{S}(\mathbf{x}) + \mathbf{B}\mathbf{u},$$
$$y = \mathbf{P}\mathbf{S}(\mathbf{x}), \tag{3}$$

where $\mathbf{x} \in R^n$ is the input vector of hidden neurons, $\mathbf{u} \in R^m$ is the control input, $\mathbf{D} = d\mathbf{I}_n$ is the constant diagonal matrix with $d > 0$. $\mathbf{A} \in R^{n\times n}$, $\mathbf{B} \in R^{n\times m}$ and $\mathbf{P} \in R^{l\times n}$ are the self-recurrent weight matrix in the hidden layer, the weight matrix between the input and hidden layers, and the weight vector between the output and hidden layers, respectively. $y \in R$ is the output of the ANN. $\mathbf{S}(\mathbf{x}) = \{s(x_1), \ldots, s(x_n)\}^{\mathrm{T}}$. Because $s(x)$ is the hyperbolic tangential function, $\|\mathbf{S}(\mathbf{x})\| \leqslant s_0$, where $s_0 > 0$ and $\|\cdot\|$ represents Frobenius norm. The recurrent neural network model shown in Fig. 1 can be viewed as an extension of the Hopfield network.

Due to the approximation capabilities of the neural network [3], it can be assumed without loss of generality that the input–output mapping of the system can be represented by a recurrent neural network mentioned above, plus an error term $\varepsilon(x, u)$. In other words, there exist ideal weight values $\mathbf{A}^* \in R^{n\times n}$, $\mathbf{B}^* \in R^{n\times m}$ and $\mathbf{P}^* \in R^{l\times n}$, which are unknown, but the matrices are constant or vary slowly with time, satisfying $\|\mathbf{A}^*\| \leqslant A_0$, $\|\mathbf{B}^*\| \leqslant B_0$ and $\|\mathbf{P}^*\| \leqslant P_0$, where A_0, B_0 and P_0 are positive constants, which enable the following system:

$$\dot{\mathbf{x}} = -\mathbf{D}\mathbf{x} + \mathbf{A}^*\mathbf{S}(\mathbf{x}) + \mathbf{B}^*\mathbf{u} + \varepsilon(x, u),$$
$$Y = \mathbf{P}^*\mathbf{S}(\mathbf{x}) \tag{4}$$

to approximate the input–output mapping of the system, where $\varepsilon(x,u)$ is the modeling error or external disturbance and $\|\varepsilon(x,u)\| \leqslant \varepsilon_0$ ($\varepsilon_0 > 0$).

For simplification, this paper assumed that desired value y_d and its derivativeness with respect to time $\dot{y}_d$ are bounded, that is $|y_d| \leqslant y_0$ and $|\dot{y}_d| \leqslant \bar{y}_0$, where $y_0 > 0$ and $\bar{y}_0 > 0$.

3. Stable adaptive control

According to the above discussion, the problem of stable adaptive neural control of the system can be described as follows: for a given proposed output $y_d(t)$, seek a control input $\mathbf{u}(t)$ to make the output Y of Eq. (4) trace the designated output with an acceptable precision and require all the signals in the closed loop to be bounded.

Suppose that $\mathbf{A}$, $\mathbf{B}$ and $\mathbf{P}$ are the approximated values of $\mathbf{A}^*$, $\mathbf{B}^*$ and $\mathbf{P}^*$, respectively. Define $\tilde{\mathbf{A}} = \mathbf{A} - \mathbf{A}^*$, $\tilde{\mathbf{B}} = \mathbf{B} - \mathbf{B}^*$ and $\tilde{\mathbf{P}} = \mathbf{P} - \mathbf{P}^*$; then Eq. (4) can be written as follows:

$$\begin{aligned} \dot{\mathbf{x}} &= -\mathbf{D}\mathbf{x} + \mathbf{A}\mathbf{S}(\mathbf{x}) + \mathbf{B}\mathbf{u} - \tilde{\mathbf{A}}\mathbf{S}(\mathbf{x}) - \tilde{\mathbf{B}}\mathbf{u} + \varepsilon(x,u), \\ Y &= \mathbf{P}\mathbf{S}(\mathbf{x}) - \tilde{\mathbf{P}}\mathbf{S}(\mathbf{x}). \end{aligned} \tag{5}$$

Denotes $s'(x) = \mathrm{d}s(x)/\mathrm{d}x$, define $\mathbf{F} = \mathrm{diag}[s'(x_1), \ldots, s'(x_n)]$ and $\mathbf{C} = \mathbf{PF}$, $\tilde{\mathbf{C}} = \tilde{\mathbf{P}}\mathbf{F}$, $\mathbf{C}^* = \mathbf{P}^*\mathbf{F}$.

In order to guarantee the stability of the control system in the sense of Lyapunov stability [25], we construct the update law on the weights in the neural network and the control inputs are as follows:

$$\dot{\mathbf{A}} = -K_a\mathbf{A} + K\mathbf{C}^{\mathrm{T}}e\mathbf{S}^{\mathrm{T}}(x), \tag{6}$$

$$\dot{\mathbf{B}} = -K_b\mathbf{B} + K\mathbf{C}^{\mathrm{T}}e\mathbf{u}^{\mathrm{T}}, \tag{7}$$

$$\dot{\mathbf{P}} = \frac{Ke(\mathbf{F}\mathbf{D}\mathbf{x})^{\mathrm{T}}}{1 + \|\mathbf{x}\|}, \tag{8}$$

$$\mathbf{u} = \frac{(\mathbf{C}\mathbf{B})^{\mathrm{T}}[\mathbf{C}\mathbf{D}\mathbf{x} + \frac{1}{\lambda}\mathbf{C}\mathbf{A}\mathbf{S}(x) + \dot{y}_d - e]}{(1 + \|\mathbf{C}\|^2\|\mathbf{B}\|^2) \cdot (1 + \|\mathbf{A}\| + \|\mathbf{x}\|)}, \tag{9}$$

where $e = z - y_d$ is the control error, z the actual output of the system, and K, K_a, K_b, λ are all positive parameters to be selected. The schematic diagram of the control system is shown in Fig. 2.

Lemma. *If Eq.* (9) *is adopted as the control law and Eqs.* (6)–(8) *as the training algorithm of the adjustable weights, then the weight matrices* $\mathbf{A}$, $\mathbf{B}$ *and* $\mathbf{P}$ *of the neural network and the input of the hidden neuron* $\mathbf{x}$ *and control input* $\mathbf{u}$ *are all bounded.*

Proof. From Eq. (8), we have

$$\|\dot{\mathbf{P}}\| = \left\| \frac{Ke(\mathbf{F}\mathbf{D}\mathbf{x})^{\mathrm{T}}}{1 + \|\mathbf{x}\|} \right\| \leqslant \frac{K|e| \cdot \|\mathbf{F}\| \cdot \|\mathbf{D}\| \cdot \|\mathbf{x}\|}{1 + \|\mathbf{x}\|} \leqslant K|e| \cdot \|\mathbf{F}\| \cdot \|\mathbf{D}\| \cdot \tag{10}$$

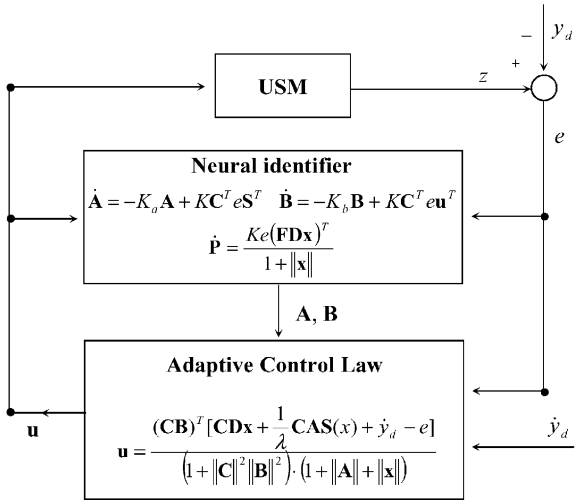

Fig. 2. Schematic diagram of the control system.

Owing to the boundedness of the output of a dynamic system and the desired value, error $e = z - y_d$ is bounded. Because e, $\mathbf{F}$ and $\mathbf{D}$ are bounded, $\dot{\mathbf{P}}$ is bounded. And the initial values of weights $\mathbf{P}$ are bounded, the weights $\mathbf{P}$, as well as weights $\tilde{\mathbf{P}}$, are still bounded after finite times updating. Then, according to the definition of $\mathbf{C}$, $\tilde{\mathbf{C}}$ and $\mathbf{C}^*$, they are all bounded. Therefore, in the following we suppose that $|\mathbf{C}| \leqslant c_0$, $|\tilde{\mathbf{C}}| \leqslant \tilde{c}_0$ and $|\mathbf{C}^*| \leqslant c_0^*$ $(c_0 > 0, \tilde{c}_0 > 0, c_0^* > 0)$.

According to Eq. (9), we have

$$
\begin{aligned}
|\mathbf{u}| &= \left|\frac{(\mathbf{CB})^{\mathrm{T}}[\mathbf{CDx} + \frac{1}{\lambda}\mathbf{CAS}(\mathbf{x}) + \dot{y}_d - e]}{(1 + \|\mathbf{C}\|^2\|\mathbf{B}\|^2)(1 + \|\mathbf{A}\| + \|\mathbf{x}\|)}\right| \\
&\leqslant \frac{\|\mathbf{C}\| \cdot \|\mathbf{D}\| \cdot \|\mathbf{x}\| + \frac{1}{\lambda}\|\mathbf{C}\| \cdot \|\mathbf{A}\| \cdot \|\mathbf{S}(\mathbf{x})\| + \|\dot{y}_d - e\|}{(1 + \|\mathbf{A}\| + \|\mathbf{x}\|)} \\
&\leqslant \frac{c_0 d\|\mathbf{x}\| + \frac{1}{\lambda}c_0 s_0\|\mathbf{A}\| + \|\dot{y}_d - e\|}{(1 + \|\mathbf{A}\| + \|\mathbf{x}\|)} \leqslant \frac{\max(c_0 d, \frac{1}{\lambda}c_0 s_0)(\|\mathbf{x}\| + \|\mathbf{A}\|) + \|\dot{y}_d - e\|}{(1 + \|\mathbf{A}\| + \|\mathbf{x}\|)} \\
&\leqslant \max\left(c_0 d, \frac{1}{\lambda}c_0 s_0\right) + \frac{\|\dot{y}_d - e\|}{(1 + \|\mathbf{A}\| + \|\mathbf{x}\|)} \leqslant \max\left(c_0 d, \frac{1}{\lambda}c_0 s_0\right) + \|\dot{y}_d\| + \|e\|. \qquad (11)
\end{aligned}
$$

Noting that e and $\dot{y}_d$ are bounded, we have the control law $\mathbf{u}$ is also bounded.

Owing to the boundedness of e, $\mathbf{u}$, $\mathbf{C}$ and $\mathbf{S}(\mathbf{x})$, from Eqs. (6) and (7) and in a similar way to the discussion of the boundedness of weights $\mathbf{P}$, it can be seen that the weights $\mathbf{A}$ and $\mathbf{B}$ are also bounded. Furthermore, from the first formula of Eq. (1), it can also be seen that the input of the hidden neuron $\boldsymbol{x}$ is bounded. This completes the proof of the lemma. □

Because $\mathbf{u}$ and $\boldsymbol{x}$ are bounded, in the following we suppose that $|\mathbf{u}| \leqslant u_0$ and $|\mathbf{x}| \leqslant x_0 (u_0 > 0, x_0 > 0)$.

Theorem. *Consider Eq.* (5). *Adopt Eq.* (9) *as the control law and Eqs.* (6)–(8) *as the training algorithm of the adjustable weights. If the positive numbers* K, K_a, λ *satisfy*

(1) $K = K_1 + K_2, K_a = K_{a1} + K_{a2}$, *where* K_1, K_2, K_{a1}, K_{a2} *are positive.*
(2) $\lambda \geqslant Kc_0s_0/(\sqrt{2K_2K_{a2}} - Kc_0s_0)$ *and* $K_2K_{a2} > (Kc_0s_0)^2/2$.

Then the trace error converges to a range near the zero point and remains within the domain throughout the execution and all signals in the closed loop are bounded.

Proof. Take the Lyapunov function as

$$L = \tfrac{1}{2}(Ke^{\mathrm{T}}e + \mathrm{tr}\{\tilde{\mathbf{A}}^{\mathrm{T}}\tilde{\mathbf{A}}\} + \mathrm{tr}\{\tilde{\mathbf{B}}^{\mathrm{T}}\tilde{\mathbf{B}}\} + \mathrm{tr}\{\tilde{\mathbf{P}}^{\mathrm{T}}\tilde{\mathbf{P}}\}) \tag{12}$$

where $\mathrm{tr}\{\cdot\}$ represents the trace of a matrix defined as $\mathrm{tr}\{\mathbf{A}^{\mathrm{T}}\mathbf{A}\} = \sum_{i,j}(a_{ij})^2 = \|\mathbf{A}\|^2$.

Differentiating Eq. (12) with respect to time, we obtain

$$\dot{L} = Ke^{\mathrm{T}}\dot{e} + \mathrm{tr}\{\dot{\tilde{\mathbf{A}}}^{\mathrm{T}}\tilde{\mathbf{A}}\} + \mathrm{tr}\{\dot{\tilde{\mathbf{B}}}^{\mathrm{T}}\tilde{\mathbf{B}}\} + \mathrm{tr}\{\dot{\tilde{\mathbf{P}}}^{\mathrm{T}}\tilde{\mathbf{P}}\}. \tag{13}$$

According to the above discussion, there exist ideal weight values $\mathbf{A}^*, \mathbf{B}^*$ and $\mathbf{P}^*$ such that the output of Eq. (5) satisfies $Y \approx z$, then we have $e = z - y_d \approx Y - y_d$. Using Eq. (4) we have

$$\dot{e} = \dot{Y} - \dot{y}_d = \mathbf{C}^*\dot{\mathbf{x}} - \dot{y}_d = \mathbf{C}^*(-\mathbf{D}\mathbf{x} + \mathbf{A}^*\mathbf{S}(\mathbf{x}) + \mathbf{B}^*\mathbf{u} + \varepsilon(x,u)) - \dot{y}_d. \tag{14}$$

Substituting Eq. (14) into Eq. (13) and noticing that $\tilde{\mathbf{A}} = \mathbf{A} - \mathbf{A}^*, \tilde{\mathbf{B}} = \mathbf{B} - \mathbf{B}^*$ and $\tilde{\mathbf{P}} = \mathbf{P} - \mathbf{P}^*$, we have

$$\begin{aligned}
\dot{L} &= Ke^{\mathrm{T}}\mathbf{C}^*(-\mathbf{D}\mathbf{x} + \mathbf{A}^*\mathbf{S}(\mathbf{x}) + \mathbf{B}^*\mathbf{u} + \varepsilon(x,u)) - Ke^{\mathrm{T}}\dot{y}_d + \mathrm{tr}\{\dot{\tilde{\mathbf{A}}}^{\mathrm{T}}\tilde{\mathbf{A}}\} + \mathrm{tr}\{\dot{\tilde{\mathbf{B}}}^{\mathrm{T}}\tilde{\mathbf{B}}\} + \mathrm{tr}\{\dot{\tilde{\mathbf{P}}}^{\mathrm{T}}\tilde{\mathbf{P}}\} \\
&= Ke^{\mathrm{T}}\mathbf{C}^*\varepsilon(x,u) + Ke^{\mathrm{T}}(\mathbf{C} - \tilde{\mathbf{C}})(-\mathbf{D}\mathbf{x} + \mathbf{A}^*\mathbf{S}(\mathbf{x}) + \mathbf{B}^*\mathbf{u}) - Ke^{\mathrm{T}}\dot{y}_d + \mathrm{tr}\{\dot{\mathbf{A}}^{\mathrm{T}}\tilde{\mathbf{A}}\} + \mathrm{tr}\{\dot{\mathbf{B}}^{\mathrm{T}}\tilde{\mathbf{B}}\} + \mathrm{tr}\{\dot{\mathbf{P}}^{\mathrm{T}}\tilde{\mathbf{P}}\} \\
&= Ke^{\mathrm{T}}\mathbf{C}^*\varepsilon(x,u) + Ke^{\mathrm{T}}\mathbf{C}(-\mathbf{D}\mathbf{x} + \mathbf{A}^*\mathbf{S}(\mathbf{x}) + \mathbf{B}^*\mathbf{u}) - Ke^{\mathrm{T}}\tilde{\mathbf{C}}(-\mathbf{D}\mathbf{x} + \mathbf{A}^*\mathbf{S}(\mathbf{x}) + \mathbf{B}^*\mathbf{u}) - Ke^{\mathrm{T}}\dot{y}_d \\
&\quad + \mathrm{tr}\{\dot{\mathbf{A}}^{\mathrm{T}}\tilde{\mathbf{A}}\} + \mathrm{tr}\{\dot{\mathbf{B}}^{\mathrm{T}}\tilde{\mathbf{B}}\} + \mathrm{tr}\{\dot{\mathbf{P}}^{\mathrm{T}}\tilde{\mathbf{P}}\} \\
&= Ke^{\mathrm{T}}\mathbf{C}^*\varepsilon(x,u) + Ke^{\mathrm{T}}\mathbf{C}(-\mathbf{D}\mathbf{x} + \mathbf{A}^*\mathbf{S}(\mathbf{x}) + \mathbf{B}^*\mathbf{u}) + Ke^{\mathrm{T}}\tilde{\mathbf{C}}\mathbf{D}\mathbf{x} + w - Ke^{\mathrm{T}}\dot{y}_d \\
&\quad + \mathrm{tr}\{\dot{\mathbf{A}}^{\mathrm{T}}\tilde{\mathbf{A}}\} + \mathrm{tr}\{\dot{\mathbf{B}}^{\mathrm{T}}\tilde{\mathbf{B}}\} + \mathrm{tr}\{\dot{\mathbf{P}}^{\mathrm{T}}\tilde{\mathbf{P}}\},
\end{aligned} \tag{15}$$

where $w = -Ke^{\mathrm{T}}\tilde{\mathbf{C}}(\mathbf{A}^*\mathbf{S}(\mathbf{x}) + \mathbf{B}^*\mathbf{u})$. Then

$$\begin{aligned}
\|w\| &= \|Ke^{\mathrm{T}}\tilde{\mathbf{C}}(\mathbf{A}^*\mathbf{S}(\mathbf{x}) + \mathbf{B}^*\mathbf{u})\| \leqslant K|e| \cdot \|\tilde{\mathbf{C}}\| \cdot (\|\mathbf{A}^*\| \cdot \|\mathbf{S}(\mathbf{x})\| + \|\mathbf{B}^*\| \cdot |\mathbf{u}|) \\
&\leqslant K|e|\tilde{c}_0(A_0s_0 + B_0u_0) = K|e|w_0,
\end{aligned} \tag{16}$$

where $w_0 = \tilde{c}_0(A_0s_0 + B_0u_0)$.

In Eq. (15), the item $Ke^{\mathrm{T}}\mathbf{C}(-\mathbf{D}\mathbf{x} + \mathbf{A}^*\mathbf{S}(\mathbf{x}) + \mathbf{B}^*\mathbf{u})$ can be written as

$$\begin{aligned}
Ke^{\mathrm{T}}\mathbf{C}(-\mathbf{D}\mathbf{x} + \mathbf{A}^*\mathbf{S}(\mathbf{x}) + \mathbf{B}^*\mathbf{u}) &= Ke^{\mathrm{T}}\mathbf{C}(-\mathbf{D}\mathbf{x} + (\mathbf{A} - \tilde{\mathbf{A}})\mathbf{S}(\mathbf{x}) + (\mathbf{B} - \tilde{\mathbf{B}})\mathbf{u}) \\
&= -Ke^{\mathrm{T}}\mathbf{C}\mathbf{D}\mathbf{x} + Ke^{\mathrm{T}}\mathbf{C}\mathbf{A}\mathbf{S}(\mathbf{x}) + Ke^{\mathrm{T}}\mathbf{C}\mathbf{B}\mathbf{u} - Ke^{\mathrm{T}}\mathbf{C}\tilde{\mathbf{A}}\mathbf{S}(\mathbf{x}) \\
&\quad - Ke^{\mathrm{T}}\mathbf{C}\tilde{\mathbf{B}}\mathbf{u}.
\end{aligned} \tag{17}$$

Substituting Eqs. (6)–(9) and (17) into Eq. (15), we have

$$\begin{aligned}\dot{L} &= Ke^{\mathrm{T}}\mathbf{C}(-\mathbf{Dx}+\mathbf{AS}(\mathbf{x})+\mathbf{Bu})+Ke^{\mathrm{T}}\mathbf{C}^{*}\varepsilon(x,u)+Ke^{\mathrm{T}}\tilde{\mathbf{C}}\mathbf{Dx}-\frac{1}{1+\|\mathbf{x}\|}Ke^{\mathrm{T}}\tilde{\mathbf{C}}\mathbf{Dx}\\ &\quad -Ke^{\mathrm{T}}\dot{y}_d-K_a\mathrm{tr}\{\mathbf{A}^{\mathrm{T}}\tilde{\mathbf{A}}\}-K_b\mathrm{tr}\{\mathbf{B}^{\mathrm{T}}\tilde{\mathbf{B}}\}+w\\ &= -Ke^{\mathrm{T}}\mathbf{CDx}+Ke^{\mathrm{T}}\mathbf{CAS}(\mathbf{x})+Ke^{\mathrm{T}}\mathbf{CB}\frac{(\mathbf{CB})^{\mathrm{T}}[\mathbf{CDx}+(1/\lambda)\mathbf{CAS}(\boldsymbol{x})+\dot{y}_d-e]}{(1+\|\mathbf{C}\|^2\|\mathbf{B}\|^2)(1+\|\mathbf{A}\|+\|\mathbf{x}\|)}+Ke^{\mathrm{T}}\mathbf{C}^{*}\varepsilon(x,u)\\ &\quad +\left(1-\frac{1}{1+\|\mathbf{x}\|}\right)Ke^{\mathrm{T}}\tilde{\mathbf{C}}\mathbf{Dx}-Ke^{\mathrm{T}}\dot{y}_d-K_a\mathrm{tr}\{\mathbf{A}^{\mathrm{T}}\tilde{\mathbf{A}}\}-K_b\mathrm{tr}\{\mathbf{B}^{\mathrm{T}}\tilde{\mathbf{B}}\}+w\\ &\leqslant -Ke^{\mathrm{T}}e+K\left(1+\frac{1}{\lambda}\right)e^{\mathrm{T}}\mathbf{CAS}(\mathbf{x})+Ke^{\mathrm{T}}\mathbf{C}^{*}\varepsilon(x,u)+\left(\frac{\|\mathbf{x}\|}{1+\|\mathbf{x}\|}\right)Ke^{\mathrm{T}}\tilde{\mathbf{C}}\mathbf{Dx}\\ &\quad -K_a\mathrm{tr}\{\mathbf{A}^{\mathrm{T}}\tilde{\mathbf{A}}\}-K_b\mathrm{tr}\{\mathbf{B}^{\mathrm{T}}\tilde{\mathbf{B}}\}+w,\end{aligned}\tag{18}$$

where the inequality $\mathbf{CB}(\mathbf{CB})^{\mathrm{T}}/(1+\|\mathbf{C}\|^2\|\mathbf{B}\|^2)<1$ is employed.

Moreover, from Ref. [17], we have

$$\mathrm{tr}(\mathbf{A}^{\mathrm{T}}\tilde{\mathbf{A}})=\tfrac{1}{2}(\|\mathbf{A}\|^2+\|\tilde{\mathbf{A}}\|^2-\|\mathbf{A}^{*}\|^2),\tag{19}$$

$$\mathrm{tr}(\mathbf{B}^{\mathrm{T}}\tilde{\mathbf{B}})=\tfrac{1}{2}(\|\mathbf{B}\|^2+\|\tilde{\mathbf{B}}\|^2-\|\mathbf{B}^{*}\|^2).\tag{20}$$

Substituting Eqs. (16), (19) and (20) into Eq. (18), we have

$$\begin{aligned}\dot{L} &\leqslant -K|e|^2+K\left(1+\frac{1}{\lambda}\right)|e|\,\|\mathbf{C}\|\,\|\mathbf{A}\|\,\|\mathbf{S}(\mathbf{x})\|+K|e|\,\|\mathbf{C}^{*}\|\,\|\varepsilon(x,u)\|+K\frac{\|\mathbf{x}\|}{1+\|\mathbf{x}\|}\cdot|e|\cdot\|\tilde{\mathbf{C}}\|\cdot\|\mathbf{D}\|\cdot|\mathbf{x}|\\ &\quad -\frac{K_a}{2}\|\mathbf{A}\|^2-\frac{K_a}{2}\|\tilde{\mathbf{A}}\|^2+\frac{K_a}{2}\|\mathbf{A}^{*}\|^2-\frac{K_b}{2}\|\mathbf{B}\|^2-\frac{K_b}{2}\|\tilde{\mathbf{B}}\|^2+\frac{K_b}{2}\|\mathbf{B}^{*}\|^2+\|w\|\\ &\leqslant -K|e|^2+K\left(1+\frac{1}{\lambda}\right)c_0s_0|e|\,\|\mathbf{A}\|+Kc_0^{*}\varepsilon_0|e|+K|e|\tilde{c}_0dx_0+K|e|w_0-\frac{K_a}{2}\|\mathbf{A}\|^2-\frac{K_b}{2}\|\mathbf{B}\|^2\\ &\quad +\frac{K_a}{2}\|\mathbf{A}^{*}\|^2+\frac{K_b}{2}\|\mathbf{B}^{*}\|^2\\ &\leqslant -K|e|^2+K\left(1+\frac{1}{\lambda}\right)c_0s_0|e|\,\|\mathbf{A}\|+K(c_0^{*}\varepsilon_0+w_0+\tilde{c}_0dx_0)|e|-\frac{K_a}{2}\|\mathbf{A}\|^2-\frac{K_b}{2}\|\mathbf{B}\|^2\\ &\quad +\frac{K_a}{2}A_0^2+\frac{K_b}{2}B_0^2\\ &= -K|e|^2+K\left(1+\frac{1}{\lambda}\right)c_0s_0|e|\,\|\mathbf{A}\|+K\bar{c}|e|-\frac{K_a}{2}\|\mathbf{A}\|^2-\frac{K_b}{2}\|\mathbf{B}\|^2+J,\end{aligned}\tag{21}$$

where $\bar{c}=c_0^{*}\varepsilon_0+w_0+\tilde{c}_0dx_0$, $J=(K_a/2)A_0^2+(K_b/2)B_0^2$.

Choosing positive numbers K_1,K_2 and K_{a1},K_{a2} to satisfy $K=K_1+K_2$ and $K_a=K_{a1}+K_{a2}$, we can re-write Eq. (21) as

$$\dot{L}\leqslant -K_1|e|^2-\left(K_2|e|^2-K\left(1+\frac{1}{\lambda}\right)c_0s_0|e|\,\|\mathbf{A}\|+\frac{K_{a2}}{2}\|\mathbf{A}\|^2\right)+K\bar{c}|e|-\frac{K_{a1}}{2}\|\mathbf{A}\|^2-\frac{K_b}{2}\|\mathbf{B}\|^2+J.\tag{22}$$

If we choose $\lambda \geqslant Kc_0s_0/(\sqrt{2K_2K_{a2}} - Kc_0s_0)$ and $K_2K_{a2} > (Kc_0s_0)^2/2$, then

$$\begin{aligned}\dot{L} &\leqslant -K_1|e|^2 - \left(\sqrt{K_2}|e| - \sqrt{\frac{K_{a2}}{2}}\|\mathbf{A}\|\right)^2 + K\bar{c}|e| - \frac{K_{a1}}{2}\|\mathbf{A}\|^2 - \frac{K_b}{2}\|\mathbf{B}\|^2 + J \\ &\leqslant -K_1|e|^2 + K\bar{c}|e| - \frac{K_{a1}}{2}\|\mathbf{A}\|^2 - \frac{K_b}{2}\|\mathbf{B}\|^2 + J. \end{aligned} \tag{23}$$

Define a range

$$\Omega_e := \{e|K_1|e|^2 - K\bar{c}|e| - J \leqslant 0\}, \tag{24}$$

$$\Omega := \left\{e|K_1|e|^2 - K\bar{c}|e| - J + \frac{K_{a1}}{2}\|\mathbf{A}\|^2 + \frac{K_b}{2}\|\mathbf{B}\|^2 \leqslant 0\right\}. \tag{25}$$

From Eqs. (24) and (25), it can be seen that $\Omega \subseteq \Omega_e$.

Defining scalar functions $H(\phi) = K_1\phi^2 - K\phi\bar{c} - J$ and $\xi_{\max} = \max(e|H(|e|) \leqslant 0)$, we have

$$\xi_{\max} = \frac{K\bar{c} + \sqrt{K^2\bar{c}^2 + 4K_1J}}{2K_1}. \tag{26}$$

Eq. (23) can be written as

$$\dot{L} \leqslant -H(|e|) - \frac{K_{a1}}{2}\|\mathbf{A}\|^2 - \frac{K_b}{2}\|\mathbf{B}\|^2. \tag{27}$$

In the following, it will be shown that the control error will converge to the range Ω_e and will remain within this range.

Let $e(t)$ be a solution corresponding to the initial condition $e(t_0)$. For the discussion later, we distinguish the following three possible cases:

Case 1: From Eqs. (23) and (24), when the error $e(t)$ is out of the range Ω_e, $H(|e|) > 0$. Hence, according to Eq. (27), we have $\dot{L} \leqslant -H(|e|) - (K_{a1}/2)\|\mathbf{A}\|^2 - (K_b/2)\|\mathbf{B}\|^2 < 0$.

Suppose that $e(t) \notin \Omega_e, \forall t \in [t_0, +\infty)$. Because $\dot{L}$ is strictly negative, there exists a time $T_0 > 0$ such that $\dot{L} \leqslant -\beta < 0$ when $t > T_0$, whereβ is a positive number. Integrating $\dot{L}$ from T_0 to t, we have $\int_{T_0}^{t} \dot{L}\,\mathrm{d}t \leqslant \int_{T_0}^{t} -\beta\,\mathrm{d}t$ and $L(t) \leqslant L(T_0) - \beta(t - T_0)$. It can be seen that $L(t) < 0$ when $t \to +\infty$. This contradicts the definition of L from Eq. (12). Therefore, $e(t)$ will converge to the range Ω_e in finite time.

Case 2: Suppose that at some time $t^* \geqslant t_1 > t_0$, it holds that $e(t)$ is such that $e(t^*) \in \Omega_e/\Omega$. In this case, we have $\dot{L} \leqslant 0$ according to Eqs. (23)–(25). Then $e(t)$ remains within the range Ω_e.

Case 3: When $e(t) \in \Omega$, we have $e(t) \in \Omega_e$ because $\Omega \subseteq \Omega_e$.

Let $e(t)$ be a solution resulting from the initial condition $e(t_0)$; to prove the uniform boundedness of $e(t)$, $\forall t > t_0$, we consider the following cases:

Case a: If $e(t_0) \notin \Omega_e$, as mentioned above, $e(t)$ will converge to the range Ω_e in finite time. Then we have $|e(t)|^2 = e^{\mathrm{T}}(t)e(t) \leqslant e^{\mathrm{T}}(t_0)e(t_0) = |e(t_0)|^2$ because Ω_e is the range near zero point.

Case b: If $e(t_0) \in \Omega_e$, $e(t)$ will be kept in the range Ω_e according to the above-mentioned cases 2 and 3. Therefore, we obtain $|e(t)| \leqslant \xi_{\max}$.

Noticing the boundedness of $\mathbf{A}, \mathbf{B}, \mathbf{P}, \mathbf{u}$ and $\boldsymbol{x}$ from lemma, we complete the proof of the theorem. □

According to the theorem, though the ideal values $\mathbf{A}^*$, $\mathbf{B}^*$ and $\mathbf{P}^*$, for the weights $\mathbf{A}$, $\mathbf{B}$ and $\mathbf{P}$, cannot be approached exactly, the control error can converge into the range Ω_e near zero and stay in that domain throughout the execution.

From the control designer's point of view, the aim of control does not render the outputs of the system to reach the reference values exactly but approximately with an acceptable precision.

According to Eq. (26) we have

$$\xi_{\max} = \frac{K\bar{c} + \sqrt{K^2\bar{c}^2 + 4K_1 J}}{2K_1} = \frac{(K_1 + K_2)\bar{c} + \sqrt{(K_1 + K_2)^2\bar{c}^2 + 4K_1 J}}{2K_1}$$
$$= \frac{1}{2}\bar{c}\left(1 + \frac{K_2}{K_1}\right) + \frac{1}{2}\sqrt{\bar{c}^2\left(1 + \frac{K_2}{K_1}\right)^2 + \frac{4J}{K_1}}. \tag{28}$$

From Eq. (28) it can be seen that if we choose larger K_1 or make the K_2/K_1 smaller, the control precision would be high. According to this principle, though the control error cannot reach zero, we can adjust the parameters K, K_1 and K_2 such that the error range Ω_e is small enough to improve the precision.

In addition, because the initial weights in the neural network may be far from the ideal weights, the control system may be unstable in the transient state of identification process. Therefore, the weights can be updated off-line in the neural network according to the static input–output information of the dynamical system or the experiential control law such as PID controller can be added in the initial stage to guarantee the stability of the control system in the transient state.

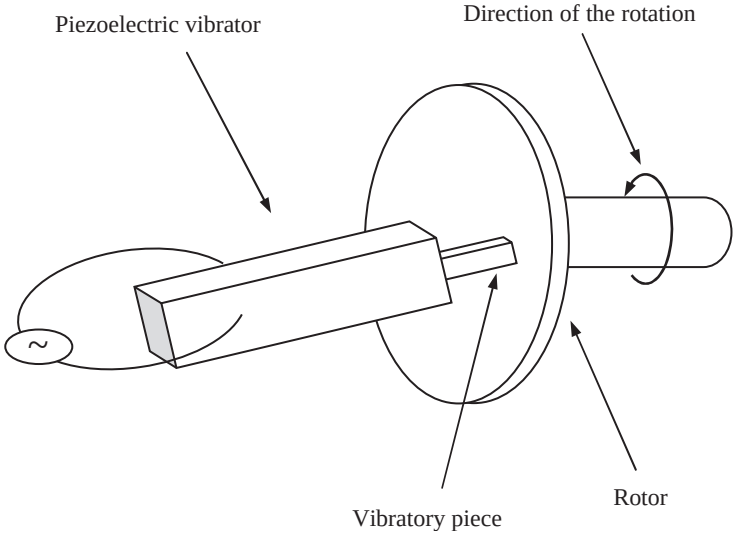

Fig. 3. Schematic diagram of the ultrasonic motor.

4. Numerical simulation results and discussion

A longitudinal vibration USM [23,26] is one of the most important USMs. In this paper, numerical simulations are performed using the proposed method for the speed control of a longitudinal vibration USM shown in Fig. 3. Some parameters of this USM model are taken as driving frequency 27.8 kHZ, amplitude of driving voltage 300 V, allowed output moment 2.5 kg cm, rotation speed 3.8 m/s.

In order to check the validity of the proposed control method, firstly the proposed speed is chosen as sinusoidal and step types. The external interferential signal $d(t) = 0.12\sin(5\pi t) + 0.05\sin^3(10\pi t) + 0.1$ is added into the output of the USM. Fig. 4(b) and (d) show the control results with the two different proposed speeds, respectively. From the figures, it can be seen that

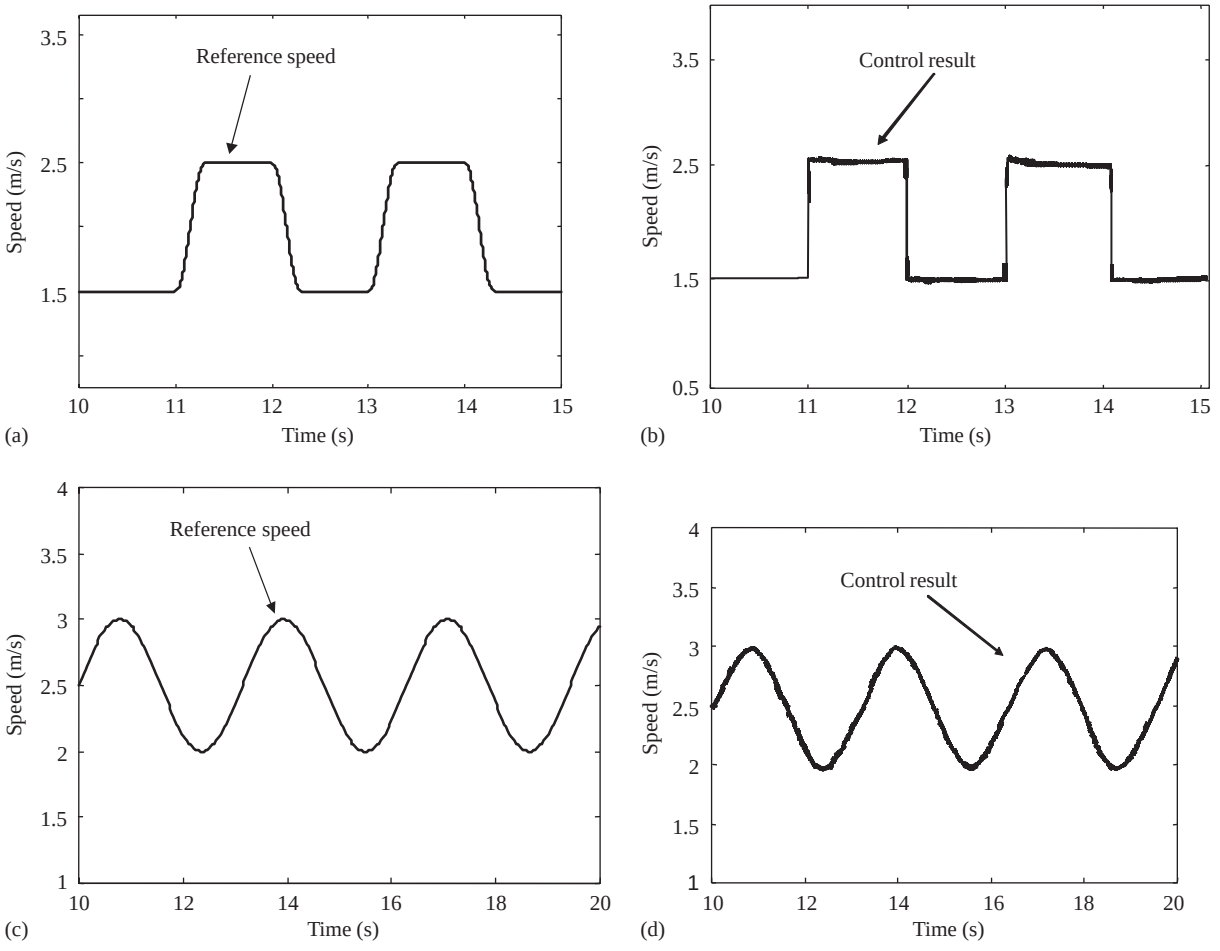

Fig. 4. Control result to different reference speeds when existing external interferential signal. (a) Reference speed with step type; (b) control result for the reference speed with step type; (c) reference speed with sinusoidal type; (d) control result for the reference speed with sinusoidal type.

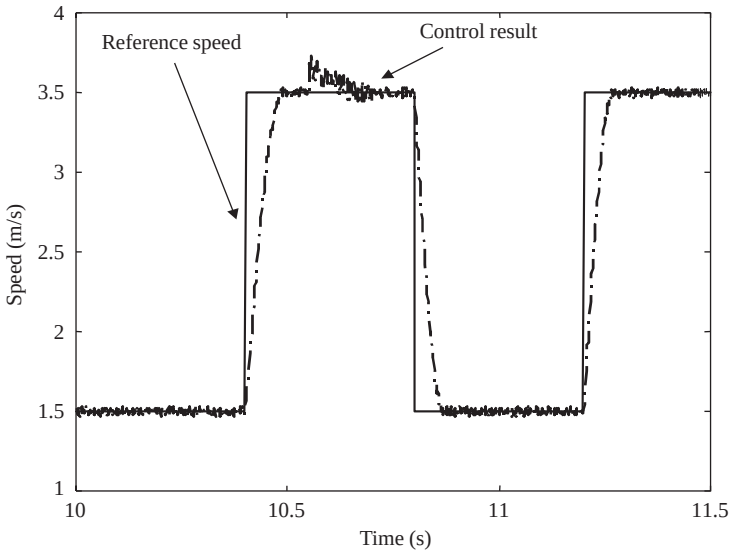

Fig. 5. Speed curve when external load changing suddenly.

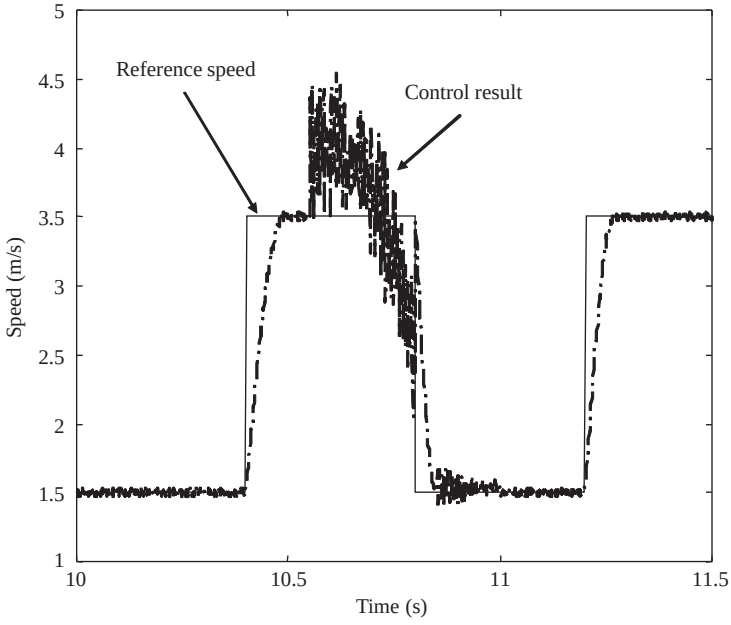

Fig. 6. Control speed curve when the parameters vary strongly.

the proposed control method can render the output of the USM converge to around the referenced value on the condition that external disturbance is exerted on the USM. Fig. 4(b) shows that the proposed control method has strong adaptive ability on the condition that the proposed value changes suddenly.

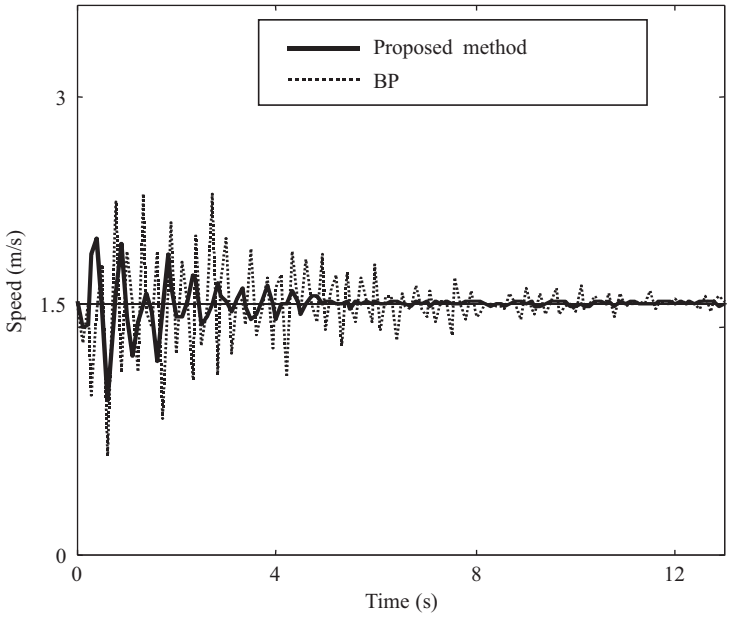

Fig. 7. Speed characteristics using different control schemes.

Fig. 5 is the speed control curve when we exert the inverse moment disturbance with amplitude of 0.2 N cm at $t \in [10.6, 12]$ s. It can be seen that the output of the USM can return to near the reference value. This shows that the proposed method has good adaptive ability when the external load changes suddenly.

Fig. 6 shows the speed control results when parameters are changed strongly for the load at 50%, elastic stiffness at 2 times and the bend modulus of elasticity at 2 times when $t > 10.6$ s. It can be seen that the proposed method can compensate for the effect of parameter variation with time. Although the strong disturbance makes the error out of zero point, the error can return near zero for a short-time control. This shows the proposed method has a good adaptive performance with respect to parameter variation.

Fig. 7 shows the comparison of the average errors using different algorithms when the desired speed value is constant. In Fig. 7, the dotted line represents the average error curve obtained using an existing neural control method [27] together with the fast adaptive learning algorithm presented in Ref. [28]. The solid line represents the results obtained using the method proposed in this paper. From Fig. 7 it can be seen that the time of convergence using the proposed method is about 6 s, which is much shorter than the time of convergence using the existing method for about 12 s. From the comparison it can be seen that the proposed method is superior to the conventional method in both control precision and convergence speed. This shows that the proposed method possesses good on-line performance. Fig. 8 shows the variation of the norm of the weights. It can be seen that the weights are bounded.

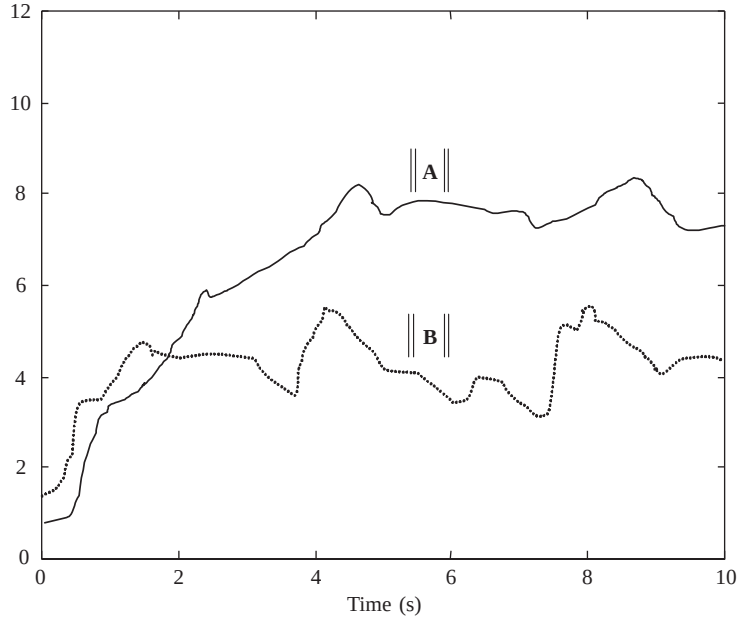

Fig. 8. Variation of $\|\mathbf{A}\|$ and $\mathbf{B}\|$.

5. Conclusions

A stable adaptive speed control scheme of nonlinear dynamical systems based on a continuous recurrent neural network is proposed. In order to guarantee stability, a newly developed algorithm of updating weights in the neural network and the control inputs are provided according to the Lyapunov stability theorem. The control error could approach a range around zero point and it keeps within the domain throughout the execution. The proposed method is examined for its on-line adapting ability, recovering ability from disturbances, and adaptive performance to parameters variation. The simulation results show that the proposed method based on the continuous recurrent neural network is promising for identification and control during on-line operation.

Acknowledgements

The first two authors and the last one are grateful to the support of the science-technology development project of Jilin Province of China (Grant No. 20030520), the key science-technology project of the National Education Ministry of China (Grant No. 02090), the doctoral funds of the National Education Ministry of China (Grant No. 20030183060), and the Key Laboratory for Symbol Computation and Knowledge Engineering of the National Education Ministry of China. The first author would also like to thank the support of the young scholarship of Mathematics College of Jilin University of China.

References

[1] J. Stoev, J.Y. Choia, J. Farrellb, Adaptive control for output feedback nonlinear systems in the presence of modeling errors, *Automatica* 38 (10) (2002) 1761–1767.

[2] V.S. Chellaboinaa, W.M. Haddadb, T. Hayakawab, Direct adaptive control for nonlinear matrix second-order dynamical systems with state-dependent uncertainty, *Systems and Control Letters* 48 (1) (2003) 53–67.

[3] S. Haykin, *Neural networks: A Comprehensive Foundation*, Prentice-Hall, Englewood Cliffs, NJ, 1999.

[4] X. Xu, Y.C. Liang, H.P. Lee, W.Z. Lin, S.P. Lim, K.H. Lee, X.H. Shi, Identification and speed control of ultrasonic motors based on neural networks, *Journal of Micromechanics and Microengineering* 13 (1) (2003) 104–114.

[5] Y.C. Liang, W.Z. Lin, H.P. Lee, S.P. Lim, K.H. Lee, D.P. Feng, A neural-network-based model reduction for dynamic simulation of MEMS, *Journal of Micromechanics and Microengineering* 11 (3) (2001) 226–233.

[6] E.N. Sanchez, L.J. Ricalde, Chaos control and synchronization, with input saturation, via recurrent neural networks, *Neural Networks* 16 (5–6) (2003) 711–717.

[7] Y.C. Liang, W.Z. Lin, H.P. Lee, S.P. Lim, K.H. Lee, H. Sun, Proper orthogonal decomposition and its application—part II: model reduction for MEMS dynamical analysis, *Journal of Sound and Vibration* 256 (3) (2002) 515–532.

[8] Y.C. Liang, D.P. Feng, J.E. Cooper, Identification of restoring forces in nonlinear vibration systems based on improved fuzzy adaptive BP algorithm, *Journal of Sound and Vibration* 242 (1) (2001) 47–58.

[9] Y.C. Liang, C.G. Zhou, Z.S. Wang, Identification of restoring forces in non-linear vibration systems based on neural networks, *Journal of Sound and Vibration* 206 (1) (1997) 103–108.

[10] G. Yagawa, H. Okuda, Neural networks in computational mechanics, *Archives of Computational Methods in Engineering—State of the Art Reviews* 3–4 (1996) 435–512.

[11] R. Le Riche, D. Gualandris, J.J. Thomas, F. Hemez, Neural identification of non-linear dynamic structures, *Journal of Sound and Vibration* 248 (2) (2001) 247–265.

[12] D. Moshou, H. Ramon, Vibration control using self-organizing look-up tables, *Journal of Sound and Vibration* 266 (3) (2003) 601–612.

[13] R.J. Wai, Tracking control based on neural network strategy for robot manipulator, *Neurocomputing* 51 (2003) 425–445.

[14] C.C. Ku, K.Y. Lee, Diagonal recurrent neural networks for dynamical systems control, *IEEE Transactions on Neural Networks* 6 (1) (1995) 144–156.

[15] F.J. Lin, R.J. Wai, C.M. Hong, Identification and control of rotary traveling-wave type ultrasonic motor using neural networks, *IEEE Transactions on Control Systems Technology* 9 (4) (2001) 672–680.

[16] X.H. Shi, Y.C. Liang, H.P. Lee, W.Z. Lin, X. Xu, S.P. Lim, Improved Elman networks and applications for controlling ultrasonic motors, *Applied Artificial Intelligence* 18(7) (2004) 603–629.

[17] G.A. Rovithakis, Robust neural adaptive stabilization of unknown systems with measurement noise, *IEEE Transactions on systems, Man, and Cybernetics—Part B: Cybernetics* 29 (3) (1999) 453–459.

[18] G.J. Kulawski, M.A. Brdysh, Stable adaptive control with recurrent networks, *Automatica* 36 (1) (2000) 5–22.

[19] J.Q. Gong, B. Yao, Neural network adaptive robust control of nonlinear systems in semi-strict feedback form, *Automatica* 37 (8) (2001) 1149–1160.

[20] T. Sashida, T. Kenjo, *An Introduction to Ultrasonic Motors*, Clarendon Press, Oxford, 1993.

[21] S. Ueha, T. Tomikawa, *Piezoelectric Motors: Theory and Application*, Oxford Science Publications, Oxford, 1993.

[22] K. Uehino, Piezoelectric motors: overview, *Smart Materials and Structures* 7 (7) (1998) 273–285.

[23] X. Xu, Y.C. Liang, H.P. Lee, W.Z. Lin, S.P. Lim, K.H. Lee, X.H. Shi, Mechanical modeling of a longitudinal oscillation ultrasonic motor and temperature effect analysis, *Smart Materials and Structures* 12 (4) (2003) 514–523.

[24] H.Y. Kim, S.K. Ha, Analysis of a disk-type stator for the piezoelectric ultrasonic motor using impedance matrix, *Journal of Sound and Vibration* 263 (3) (2003) 643–663.

[25] C.D. Richard, H.B. Robert, *Modern Control Systems*, Higher Education Press, Beijing, 1998.

[26] T. Sashida, Trial construction and operation of an ultrasonic vibration driven motor: theoretical and experimental investigation of its performances, *Oyo Buturi* 51 (1982) 713–720 (in Japanese).

[27] T. Senjyu, H. Miyazato, S. Yokoda, K. Uezato, Speed control of ultrasonic motors using neural network, *IEEE Transactions on Power Electronics* 13 (3) (1998) 381–387.

[28] M. Riedmiller, H.A. Braun, A direct adaptive method for faster backpropagation learning: the RPROP algorithm, *Proceedings of IEEE International Conference on Neural Networks*, San Francisco, CA, 1993, pp. 586–591.